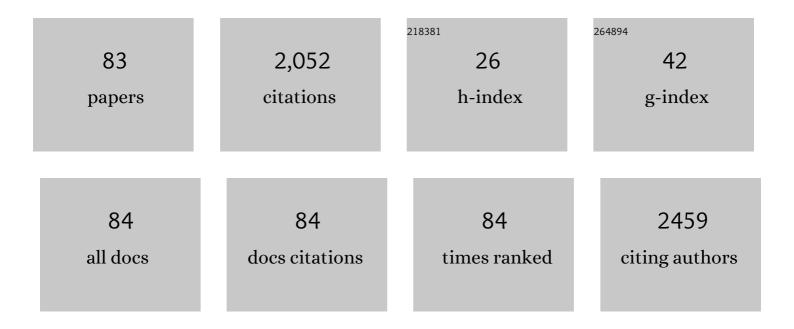
List of Publications by Year in descending order

Source: https://exaly.com/author-pdf/6143170/publications.pdf Version: 2024-02-01



#	Article	IF	CITATIONS
1	A PEM fuel cell with metal foam as flow distributor. Energy Conversion and Management, 2012, 62, 14-21.	4.4	135
2	Effects of microstructure characteristics of gas diffusion layer and microporous layer on the performance of PEMFC. Energy Conversion and Management, 2010, 51, 677-684.	4.4	134
3	Effects of flow field design on the performance of a PEM fuel cell with metal foam as the flow distributor. International Journal of Hydrogen Energy, 2012, 37, 13060-13066.	3.8	125
4	Rechargeable Na/Na0.44MnO2 cells with ionic liquid electrolytes containing various sodium solutes. Journal of Power Sources, 2015, 274, 1016-1023.	4.0	102
5	Thermal conductivity of polyurethane foams from room temperature to 20 K. Cryogenics, 1997, 37, 305-312.	0.9	99
6	Revisiting graphene–polymer nanocomposite for enhancing anticorrosion performance: a new insight into interface chemistry and diffusion model. Nanoscale, 2018, 10, 12612-12624.	2.8	82
7	Effects of hydrogen addition on methane combustion in a porous medium burner. International Journal of Hydrogen Energy, 2002, 27, 699-707.	3.8	67
8	Thermal radiative properties of phenolic foam insulation. Journal of Quantitative Spectroscopy and Radiative Transfer, 2002, 72, 349-359.	1.1	64
9	Photoelectrochemical properties of AgInS2 thin films prepared using electrodeposition. Solar Energy Materials and Solar Cells, 2011, 95, 453-461.	3.0	57
10	Characterization of Pt-Cu binary catalysts for oxygen reduction for fuel cell applications. Materials Chemistry and Physics, 2006, 100, 385-390.	2.0	53
11	Combustion of Liquid Fuels in a Porous Radiant Burner. Combustion Science and Technology, 1996, 112, 141-161.	1.2	44
12	The thermal conductivity mechanism of sewage sludge ash lightweight materials. Cement and Concrete Research, 2005, 35, 803-809.	4.6	44
13	Fabrication of anode-supported thin BCZY electrolyte protonic fuel cells using NiO sintering aid. International Journal of Hydrogen Energy, 2019, 44, 23784-23792.	3.8	42
14	Electrical and optical properties of TiO2-doped ZnO films prepared by radio-frequency magnetron sputtering. Journal of Physics and Chemistry of Solids, 2008, 69, 535-539.	1.9	41
15	Application of metal foams to high temperature PEM fuel cells. International Journal of Hydrogen Energy, 2016, 41, 16196-16204.	3.8	39
16	Self-oriented iron oxide nanorod array thin film for photoelectrochemical hydrogen production. International Journal of Hydrogen Energy, 2012, 37, 13616-13622.	3.8	38
17	Preparation of TiO2-doped ZnO films by radio frequency magnetron sputtering in ambient hydrogen–argon gas. Applied Surface Science, 2008, 255, 2494-2499.	3.1	37
18	The influence of titanium on the properties of zinc oxide films deposited by radio frequency magnetron sputtering. Applied Surface Science, 2008, 254, 2615-2620.	3.1	36

#	Article	IF	CITATIONS
19	Photoelectrochemical performance of gallium-doped AgInS2 photoelectrodes prepared by electrodeposition process. Solar Energy Materials and Solar Cells, 2012, 96, 33-42.	3.0	35
20	Perovskite LSCM impregnated with vanadium pentoxide for high temperature carbon dioxide electrolysis. Electrochimica Acta, 2016, 212, 32-40.	2.6	32
21	Highly concentrated carbonate electrolyte for Li-ion batteries with lithium metal and graphite anodes. Journal of Power Sources, 2020, 450, 227657.	4.0	32
22	BaZr0.2Ce0.8â^'xYxO3â^´Î´ solid oxide fuel cell electrolyte synthesized by sol–gel combined with composition-exchange method. International Journal of Hydrogen Energy, 2014, 39, 14434-14440.	3.8	30
23	Preparation of PtSn/C electrocatalysts with improved activity and durability toward oxygen reduction reaction by alcohol-reduction process. Materials Chemistry and Physics, 2012, 135, 395-400.	2.0	29
24	Strontium doping effect on phase homogeneity and conductivity of Ba1â ``xSrxCe0.6Zr0.2Y0.2O3â ``δ proton-conducting oxides. International Journal of Hydrogen Energy, 2013, 38, 11097-11103.	3.8	29
25	Manipulation of Heteroatom Substitution on Nitrogen and Phosphorus Co-Doped Graphene as a High Active Catalyst for Hydrogen Evolution Reaction. Journal of Physical Chemistry C, 2019, 123, 22202-22211.	1.5	29
26	Ordered porous carbon as the catalyst support forÂproton-exchange membrane fuel cells. International Journal of Hydrogen Energy, 2013, 38, 10998-11003.	3.8	27
27	Graphene as corrosion protection for metal foam flow distributor in proton exchange membrane fuel cells. International Journal of Hydrogen Energy, 2017, 42, 22201-22207.	3.8	27
28	Thermodynamic analysis of a photoelectrochemical hydrogen production system. International Journal of Hydrogen Energy, 2010, 35, 2781-2785.	3.8	23
29	Review on the preparation of electrolyte thin films based on cerate-zirconate oxides for electrochemical analysis of anode-supported proton ceramic fuel cells. Journal of Alloys and Compounds, 2022, 918, 165434.	2.8	23
30	Pulsed Laser Deposition of Platinum Nanoparticles as a Catalyst for High-Performance PEM Fuel Cells. Catalysts, 2016, 6, 180.	1.6	22
31	Electrochemical Na ⁺ storage properties of SnO ₂ /graphene anodes in carbonate-based and ionic liquid electrolytes. Journal of Materials Chemistry A, 2017, 5, 13776-13784.	5.2	21
32	MoS _{<i>x</i>} on Nitrogen-Doped Graphene for High-Efficiency Hydrogen Evolution Reaction: Unraveling the Mechanisms of Unique Interfacial Bonding for Efficient Charge Transport and Stability. ACS Applied Materials & Interfaces, 2020, 12, 34825-34836.	4.0	20
33	CuFe electrocatalyst for hydrogen evolution reaction in alkaline electrolysis. International Journal of Hydrogen Energy, 2021, 46, 35886-35895.	3.8	20
34	Planar Heterojunction Solar Cell Employing a Single-Source Precursor Solution-Processed Sb ₂ S ₃ Thin Film as the Light Absorber. ACS Omega, 2019, 4, 11380-11387.	1.6	19
35	Synthesis and characterization of Ba0.6Sr0.4Ce0.8â^'xZrxY0.2O3â^'î´ proton-conducting oxides for use as fuel cell electrolyte. Journal of Alloys and Compounds, 2014, 586, S506-S510.	2.8	17
36	Nanocrystalline Pd/carbon nanotube composites synthesized using supercritical fluid for superior glucose sensing performance. Journal of Alloys and Compounds, 2014, 615, S496-S500.	2.8	17

#	Article	IF	CITATIONS
37	Electrochemical performance of 0.5Li2MnO3–0.5Li(Mn0.375Ni0.375Co0.25)O2 composite cathode inÂpyrrolidinium-based ionic liquid electrolytes. Journal of Power Sources, 2015, 294, 22-30.	4.0	16
38	Microstructures and electrical properties of zirconium doped barium cerate perovskite proton conductors. International Journal of Hydrogen Energy, 2019, 44, 21174-21180.	3.8	16
39	A triple (eâ^'/O2â^'/H+) conducting perovskite BaCo0.4Fe0.4Zr0.1Y0.1O3-δ for low temperature solid oxide fuel cell. International Journal of Hydrogen Energy, 2021, 46, 9767-9774.	3.8	16
40	The oxygen reduction reaction of ordered porous carbon-supported PtSn catalysts. RSC Advances, 2016, 6, 44205-44211.	1.7	15
41	The reactor design for photoelectrochemical hydrogen production. International Journal of Hydrogen Energy, 2011, 36, 6510-6518.	3.8	14
42	Proton-conducting Ba1â^'xKxCe0.6Zr0.2Y0.2O3â^'î´ oxides synthesized by sol–gel combined with composition-exchange method. Ceramics International, 2014, 40, 1865-1872.	2.3	14
43	Potassium doping optimization in proton-conducting Ba1-xKxCe0.6Zr0.2Y0.2O3-Î′ oxides for fuel cell applications. Journal of Alloys and Compounds, 2017, 696, 251-256.	2.8	14
44	High Durability of Pt ₃ Sn/Graphene Electrocatalysts toward the Oxygen Reduction Reaction Studied with In Situ QEXAFS. ACS Applied Materials & Interfaces, 2020, 12, 24710-24716.	4.0	14
45	Production of high-performance and improved-durability Pt-catalyst /support for proton-exchange-membrane fuel cells with pulsed laser deposition. Journal Physics D: Applied Physics, 2016, 49, 255601.	1.3	13
46	Production of La0.6Sr0.4Co0.2Fe0.8O3-Î [^] cathode with graded porosity for improving proton-conducting solid oxide fuel cells. Ceramics International, 2019, 45, 22479-22485.	2.3	13
47	Correlation between microstructure and catalytic and mechanical properties during redox cycling for Ni-BCY and Ni-BCZY composites. Ceramics International, 2017, 43, S671-S674.	2.3	12
48	Effects of TiO2 and SDC addition on the properties of YSZ electrolyte. International Journal of Hydrogen Energy, 2019, 44, 29426-29431.	3.8	12
49	Conduction-radiation interaction in absorbing, emitting, and anisotropically scattering media with variable thermal conductivity. Journal of Thermophysics and Heat Transfer, 1992, 6, 537-540.	0.9	11
50	Thermal properties of phenolic foam insulation. Journal of the Chinese Institute of Engineers, Transactions of the Chinese Institute of Engineers,Series A/Chung-kuo Kung Ch'eng Hsuch K'an, 2002, 25, 753-758.	0.6	11
51	Fractal permeability models for the microporous layer and gas diffusion layer of PEM fuel cell. Journal of the Chinese Institute of Engineers, Transactions of the Chinese Institute of Engineers,Series A/Chung-kuo Kung Ch'eng Hsuch K'an, 2011, 34, 39-47.	0.6	11
52	Redox-reversible perovskite ferrite cathode for high temperature solid oxide steam electrolyser. Electrochimica Acta, 2017, 229, 48-54.	2.6	11
53	Effects of assembling method and force on the performance of protonâ€exchange membrane fuel cells with metal foam flow field. International Journal of Energy Research, 2020, 44, 9707-9713.	2.2	11
54	Study on the surface segregation of mixed ionicâ€electronic conductor lanthanumâ€based perovskite oxide <scp> La _{1â^x} Sr _x Co _{1â^y} Fe _y O _{3â^'} </scp> _δ materials. International Journal of Energy Research, 2022, 46, 7101-7117.	2.2	10

#	Article	IF	CITATIONS
55	Hydrogen Scooter Testing and Verification Program. Energy Procedia, 2012, 29, 633-643.	1.8	9
56	Effects of zirconium oxide on the sintering of SrCe1â^'xZrxO3â~'δ (0.0≦x≦0.5). Journal of Alloys and Compounds, 2014, 615, S491-S495.	2.8	9
57	Transient combined conduction and radiation in an absorbing, emitting and anisotropically-scattering medium with variable thermal conductivity. International Journal of Heat and Mass Transfer, 1992, 35, 1844-1847.	2.5	8
58	Mechanical Properties of Ba1-xKxCe0.6Zr0.2Y0.2O3-δOxides by Nanoindentation. Procedia Engineering, 2014, 79, 599-605.	1.2	8
59	Chemical stability and electrical and mechanical properties of BaZrxCe0.8-xY0.2O3 with CeO2 protection method. International Journal of Hydrogen Energy, 2017, 42, 22259-22265.	3.8	8
60	Thermal Performance of Ultra-Fine Powder Insulations at High Temperatures. Journal of Thermal Insulation, 1989, 12, 298-312.	0.2	7
61	Numerical analysis of the solar reactor design for a photoelectrochemical hydrogen production system. International Journal of Hydrogen Energy, 2012, 37, 13053-13059.	3.8	7
62	Analysis of an intermediate-temperature proton-conducting SOFC hybrid system. International Journal of Green Energy, 2016, 13, 1640-1647.	2.1	7
63	Ba1â^xSrxCe0.8â^yZryY0.2O3â [~] î [^] protonic electrolytes synthesized by hetero-composition-exchange method for solid oxide fuel cells. International Journal of Hydrogen Energy, 2017, 42, 22222-22227.	3.8	7
64	Raising the maximum power density of nanoporous catalyst film-based polymer-electrolyte-membrane fuel cells by laser micro-machining of the gas diffusion layer. Journal of Power Sources, 2019, 436, 226886.	4.0	6
65	Nano-fibrous SrCeO·8YO·2O3-δ-Ni anode functional layer for proton-conducting solid oxide fuel cells. Journal of Power Sources, 2019, 436, 226863.	4.0	6
66	New insights into interface charge-transfer mechanism of copper-iron layered double hydroxide cathodic electrocatalyst in alkaline electrolysis. Journal of Environmental Chemical Engineering, 2022, 10, 107287.	3.3	6
67	Combined Conduction and radiation in absorbing, emitting and anisotropically-scattering, concentric, spherical media. Journal of Quantitative Spectroscopy and Radiative Transfer, 1991, 46, 251-257.	1.1	5
68	Characteristics of NixFe1â^'xOy Electrocatalyst on Hematite as Photoanode for Solar Hydrogen Production. Catalysts, 2017, 7, 350.	1.6	4
69	Supercapacitive performance of porous graphene nanosheets in bis(trifluoromethylsulfony)imide and bis(fluorosulfonyl)imide ionic liquid electrolytes. Journal of Solid State Electrochemistry, 2018, 22, 2197-2203.	1.2	4
70	Simulation of thermally-enhanced combustion in a porous medium burner. Heat Transfer - Asian Research, 2006, 35, 75-88.	2.8	3
71	Effect of the reactive surface area of proton-conducting Ni Ba0.8Sr0.2Ce0.6Zr0.2Y0.2O3-δ anodes on cell performance. Ceramics International, 2019, 45, 14524-14532.	2.3	3
72	An In Situ Quick Xâ€ray Absorption Spectroscopy Study on Pt 3 Sn/Graphene Catalyst for Ethanol Oxidation Reaction. ChemCatChem, 2021, 13, 382-387.	1.8	3

5

#	Article	IF	CITATIONS
73	Nanomechanical Properties and Fracture Behaviors of Ba1–xKxCe0.6Zr0.2Y0.2O3–δElectrolytes by Nanoindentation. Science of Advanced Materials, 2014, 6, 1691-1696.	0.1	3
74	Combined natural convection and radiation with temperature-dependent properties. Thermal Science, 2018, 22, 921-930.	0.5	3
75	Thermal stability of Ni(Ta) silicide films on ultra-thin silicon-on-insulator substrates. Journal of Alloys and Compounds, 2012, 536, S407-S411.	2.8	2
76	Preparation and characterization of high temperature Sr(Ce0.6Zr0.4)0.9Y0.1O3-Î′/YBaCo2O5+δ mixed proton-electron composite membrane. International Journal of Hydrogen Energy, 2019, 44, 29547-29553.	3.8	2
77	Performance enhancement of polymer electrolyte membrane fuel cell by PtCo3 nanoporous film as high mass-specific power density catalyst using laser deposition and processing. International Journal of Hydrogen Energy, 2021, 46, 33948-33956.	3.8	2
78	Hierarchical Carbon Composites for Highâ€Energy/Powerâ€Density and Highâ€Reliability Supercapacitors with Low Aging Rate. ChemSusChem, 2022, 15, .	3.6	2
79	Analysis of Radiative Heat Transfer in Ultra-Fine Powder Insulations Under Variation of Radiative Boundary Conditions. Journal of Thermal Insulation, 1988, 12, 108-123.	0.2	1
80	X-ray analyses and crystallography data of NiO – BaCeâ,€.54Zrâ,€.36Y0.1O2.95 composite anode for protonic ceramic fuel cell. Materials Today: Proceedings, 2022, 66, 3989-3992.	0.9	1
81	A Concept of Vertical Takeoff Two-Stage-to-Orbit Reusable Launch Vehicle with an Integral-Rocket-Ramjet Booster. Journal of Mechanics, 2005, 21, 51-56.	0.7	0
82	Creating electronic and ionic conductivity gradients for improving energy storage performance of ruthenium oxide electrodes. Journal of Alloys and Compounds, 2021, 862, 158013.	2.8	0
83	Pengaruh Doping Cu terhadap Karakteristik Material dan Ketahanan Karbon pada Anoda Ni1-X-CuX-BCZY untuk PSOFC. Rekayasa Mesin, 2020, 11, 441-447.	0.2	0